ADVANCED FUNCTIONAL MATERIALS
www.afm-journal.de

Triboelectric Nanogenerator Networks Integrated with Power Management Module for Water Wave Energy Harvesting

Xi Liang, Tao Jiang, Guoxu Liu, Tianxiao Xiao, Liang Xu, Wei Li, Fengben Xi, Chi Zhang, and Zhong Lin Wang**

Ocean waves are one of the most promising renewable energy sources for large-scope applications. Recently, triboelectric nanogenerator (TENG) network has been demonstrated to effectively harvest water wave energy possibly toward large-scale blue energy. However, the absence of effective power management severely restricts the practicability of TENGs. In this work, a hexagonal TENG network consisting of spherical TENG units based on spring-assisted multilayered structure, integrated with a power management module (PMM), is constructed for harvesting water wave energy. The output performance of the TENG network is found to be determined by water wave frequencies and amplitudes, as well as the wave type. Moreover, with the implemented PMM, the TENG network could output a steady and continuous direct current (DC) voltage on the load resistance, and the stored energy is dramatically improved by up to 96 times for charging a capacitor. The TENG network integrated with the PMM is also applied to effectively power a digital thermometer and a wireless transmitter. The thermometer can constantly measure the water temperature with the water wave motions, and the transmitter can send signals that enable an alarm to go off once every 10 s. This study extends the application of the power management module in the water wave energy harvesting.

1. Introduction

With the development of human society, energy is always a key topic because of its indispensable role for people's life. In recent years, climate deterioration and energy crisis caused by the consumption of fossil fuels have attracted worldwide attention.[1,2] It is highly urgent to search for other renewable and clean energy sources. Water wave energy, which has abundant reserves and little dependence on environmental conditions, is a promising renewable energy source with great potential for large-scale applications.[3–5] However, such energy has rarely been exploited due to lack of economical energy scavenging technologies in spite of the great efforts devoted.[6–8] So far, most demonstrated converters for water wave energy rely on the electromagnetic generators, which are heavy, bulky, costly, easily corroded, and inefficient at ocean wave frequency.[9,10] Hence, a lightweight, small-sized, cost-effective, and all-in-one approach for harvesting the water wave energy is greatly desirable.

Triboelectric nanogenerator (TENG) has provided an effective route for converting ambient mechanical energy into electricity, with unique merits of high power density, high efficiency, low weight, and low fabrication cost.[11–17] Through the coupling of triboelectrification and electrostatic induction, the TENGs can harvest energy from a variety of sources, such as human walking,[18] mechanical vibration,[19] rotation,[20] wind,[21] and water waves.[22–30] The TENGs exhibit obvious advantages over electromagnetic generators at low frequency, due to their fundamental differences in the physical mechanisms,[31,32] demonstrating the possible killer application of TENG in harvesting low-frequency energy from motions such as ocean waves.[33] In 2014, Wang proposed an idea of using TENG networks to harvest large-scale water wave energy,[34] which are made of millions of spherical ball based TENG units connected as fishing net.[5] So far, a TENG network based on fully enclosed box-like device with self-restorable arch-shaped TENGs and a coupled TENG network composed of rolling spherical TENGs have been constructed in our previous works.[22,35] Recently, the performance of single spherical TENG unit in the network has been dramatically optimized by introducing the spring-assisted multilayered structure, and a small network has also been fabricated to harness the water wave energy.[36] Nevertheless, the TENG networks have difficulties in directly powering electronics or charging storages for the large impedance and unbalanced load matching.[37–39] Therefore,

X. Liang, Prof. T. Jiang, G. Liu, T. Xiao, Prof. L. Xu, Prof. W. Li, F. Xi, Prof. C. Zhang, Prof. Z. L. Wang
CAS Center for Excellence in Nanoscience
Beijing Key Laboratory of Micro-Nano Energy and Sensor
Beijing Institute of Nanoenergy and Nanosystems
Chinese Academy of Sciences
Beijing 100083, China
E-mail: czhang@binn.cas.cn; zlwang@gatech.edu
X. Liang, Prof. T. Jiang, G. Liu, T. Xiao, Prof. L. Xu, F. Xi, Prof. C. Zhang, Prof. Z. L. Wang
School of Nanoscience and Technology
University of Chinese Academy of Sciences
Beijing 100049, China
Prof. Z. L. Wang
School of Materials Science and Engineering
Georgia Institute of Technology
Atlanta, GA 30332-0245, USA

DOI: 10.1002/adfm.201807241

effective power management is very necessary to break through this bottleneck and achieve more efficient utilization of water wave energy.

In the present work, we designed and fabricated a hexagonal TENG network by using spherical TENG units based on spring-assisted multilayered structure for harvesting water wave energy, and managed the output energy through integrating with a power management module (PMM). First, the output performance of the TENG network was systematically measured in water as triggered by real water waves under different water wave conditions. The influences of the water wave frequency and amplitude were investigated for three types of water waves, i.e., transverse sinusoidal wave, transverse impulse wave, and longitudinal impulse wave. Then the TENG network was integrated with the PMM, and the output characteristics on the load resistance and capacitance were respectively investigated. A steady and continuous direct current (DC) voltage on the load resistance was received, and the direct and managed charging speeds to a capacitor were compared. Finally, the TENG network integrated with the PMM was applied to power a digital thermometer and a wireless transmitter, demonstrating the advantage and necessity of the TENG and PMM toward large-scale blue energy harvesting.

2. Results and Discussion

A hexagonal TENG network was fabricated by using spherical TENG units, which have the spring-assisted multilayered structure as schematically illustrated in **Figure 1**a. The internal structure of the spherical unit is the same as that reported in our previous work.[36] For the spring-assisted structure; four flexible springs adhered on bottom acrylic block support the mass block, while four rigid springs attached on the top side of mass block utilize the resilience force to press the multilayered TENG. In the multilayered structure with increased space utilization, a 50 µm thick Kapton film shaped into a zigzag structure serves as the substrate of TENG basic units. The local structure of the multilayered TENG can be viewed from the enlarged figure at the right side of Figure 1a. Each basic TENG unit is based on the contact-separation between the aluminum (Al) electrode and polarized fluorinated ethylene propylene (FEP) film bonded by another aluminum electrode. The copper mass and basic unit number for each sphere are fixed as 100 g and 7 in this work. The fabrication details can be found in the Experimental Section. Figure 1b shows the working principle of each TENG unit. Under the triggering of water waves, the contact between Al and FEP film generates opposite charges on the Al and FEP surface. Then their separation produces an electric potential difference between electrodes driving the free electron flow at the external circuit. The periodic contact-separation will generate periodic alternating current. Our TENGs with the spring-assisted and multilayered structure have a much higher output current than previous water wave-driven TENGs, because of the contact-separation working mode of the TENGs with the help of the springs and the integration of multiple basic units. Then one spherical TENG can realize a higher power output (a maximum power of 7.96 mW).[36]

Figure 1c presents the schematic diagram of the hexagonal TENG network with seven TENG units linked by rigid strings

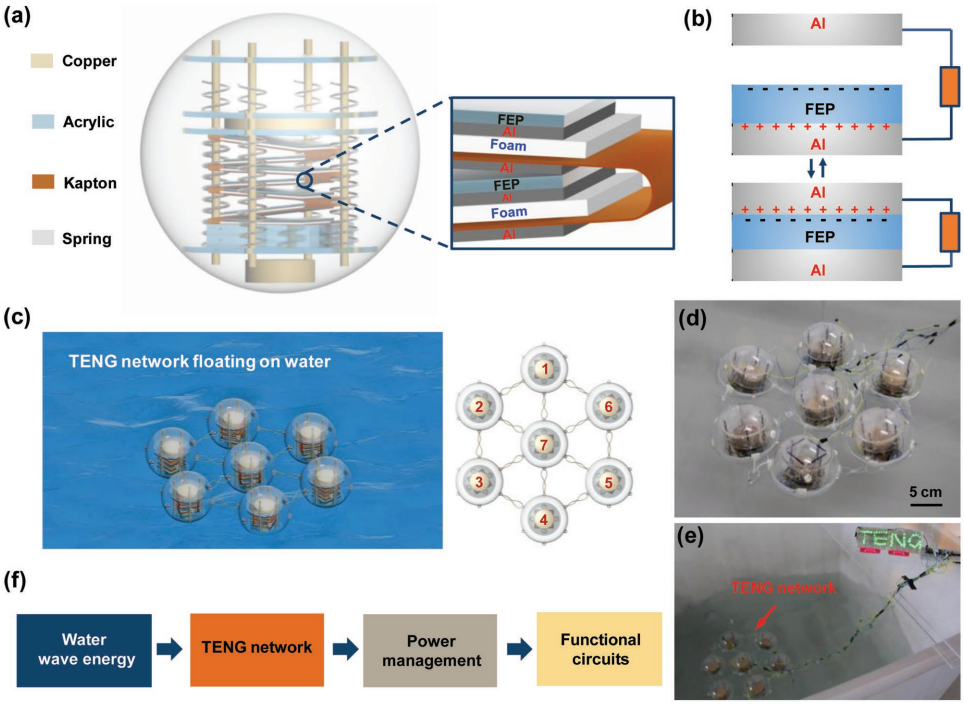

Figure 1. a) Schematic diagram of a single spherical TENG unit with spring-assisted multilayered structure, and schematic representation for local enlarged structure of the multilayered TENG with seven basic units. b) Working principle of each TENG unit of the spherical TENG. c) Schematic diagram of the hexagonal TENG network with seven TENG units linked by rigid strings floating on the water surface. The right side shows the top view of the network. d) Photograph of as-fabricated TENG network device on the water surface. e) Photograph of dozens of LEDs with a "TENG" pattern which are lighted up by the TENG network under the water wave motions. f) Framework for the integrated self-powered system driven by the water wave motions.

floating on the water surface. In the network, one unit locates in the center of the hexagon, and six units locate at the apexes of the hexagon. The top view at the right side shows the structure details of string connections. Figure 1d shows the photograph of as-fabricated TENG network device on the water surface. The seven spherical units are linked by cable ties and connected electrically in parallel. In a single spherical TENG, all the basic units are able to move synchronously, because they are pressed by the same copper block. However, the motion phase sameness in the TENG array is difficult to be fully realized due to the different motion states of spherical TENGs under the water wave movements. If the electrodes of spherical TENG units are directly connected, the interference of multiple signals will destructively impact the output performance. To avoid the interference, we connected the spherical TENG units through seven rectifier bridges respectively. In this way, the energy harvested by the TENG network was not offset.[40] Under the water wave motions, dozens of light-emitting diodes (LEDs) with a "TENG" pattern can be lighted up by the TENG network, as viewed from Figure 1e. The wave type is the transverse sinusoidal wave. For practical applications, an integrated self-powered system driven by the water wave motions needs to be constructed. The system framework is illustrated in Figure 1f, including a water-wave-driven TENG network and functional circuits for different applications. The TENG network harvests water wave energy and produces alternating-current (AC) electric outputs, which will be converted into a steady DC output by the power management module. The DC electricity can directly power diversified functional circuits, such as sensors, displays, and wireless transmitters, or power the circuits through the energy storage. These signals collected by sensors are visualized on a liquid crystal displayer (LCD) or sent out through a wireless transmitter.

The external water wave conditions, such as the wave type, frequency, and amplitude of the water waves are important factors influencing the output performance of TENG network. When we placed the TENG network into the water tank, we applied a function generator to drive a series of wave pumps to generate different water waves. For the water wave type, the transverse sinusoidal wave, the transverse impulse wave and the longitudinal impulse wave were considered. The motion manners for the units in the hexagonal TENG network were compared for three types of waves, which can be viewed from Video S1 Supporting Information. Triggered by the three waves, the LEDs could all be lighted up, but had different brightness dependent on the network output. The rectified output characteristics of the TENG network were measured at different frequencies of water waves from 0.5 to 2.0 Hz for the three types of water waves, as shown in **Figure 2**. Actual ocean waves are usually at a low frequency below 2.0 Hz, so we selected the frequency range of water waves from 0.5 to 2.0 Hz for instance to investigate the influence of wave frequency. The output voltage amplitude H_{out} of the function generator was fixed as 2.5 V. Due to the instability of water waves, the accurate wave amplitude (wave height) is difficult to be measured directly. In this work, the amplitude H_{out} was adopted as a variable to reflect amplitude of water waves, because it is approximately proportional to the water wave amplitude.

Figure 2a–c shows the rectified output current, voltage and the power–resistance relationship of the TENG network device as functions of the water wave frequency under the transverse sinusoidal waves. The current and voltage were expected to be measured under the short-circuit condition and open-circuit condition, respectively. However, due to the internal impedance of current preamplifier and internal resistance of digital oscilloscope, we could not obtain the real short-circuit current and open-circuit voltage. So we called them as output current and output voltage. As the water wave frequency increases, the peak values of the output current and output voltage both first increase and then decrease, exhibiting the maximum values of 78 μA and 253 V at the frequency of 1.5 Hz. When the frequency is higher than 1.5 Hz, the vibration period is not long enough for the mass block to press the TENG part sufficiently, leading to the drop of the electric outputs. The instantaneous output power of the network also reaches the maximum value of 4.31 mW at 1.5 Hz, and the matched resistance is 3.3 MΩ. When the wave type becomes from transverse sinusoidal to transverse impulse, the rectified outputs of the TENG network have slight changes, and the optimal frequency decreases from 1.5 to 1.0 Hz (Figure 2d–f). The maximum current and voltage are 97 μA and 257 V, and the power reaches 4.27 mW at the resistance of 2.8 MΩ. Note that a spherical TENG unit hardly works in the transverse water waves, so clearly the linkage between the units changes the motion mode of the spherical TENGs. For the longitudinal impulse waves, the outputs of the TENG network are the highest, delivering the maximum power of 12.20 mW (3.33 W m^{-3}) at the matched resistance of 1.2 MΩ (Figure 2g–i). The current of 270 μA and voltage of 354 V were obtained at the optimal frequency of 1.0 Hz. It can be found that the vertical wave impact can induce the TENG network to generate higher outputs, but the common transverse water waves can also realize the wave energy conversion.

Subsequently, we investigated the influence of the water wave amplitude on the output performance of the TENG network under these three types of water waves. Under the transverse sinusoidal waves, the trends of the output current and output voltage with respect to the H_{out} varying from 1.0 to 2.5 V are shown in **Figure 3**a,b. The water wave frequency was fixed at 1.5 Hz, since it is the optimal frequency (Figure 2a–c). As it can be seen, the output current and voltage both increase with increasing the H_{out}. Compared to the outputs at H_{out} = 1.0 V, the output current and voltage at H_{out} = 2.5 V are enhanced by 3.57 times and 0.67 times, respectively. Figure 3c shows the output power of the TENG network as a function of the load resistance at different H_{out} under the transverse sinusoidal waves. The maximum output power at H_{out} = 2.5 V has an enhancement of 18.75 times over the power at H_{out} = 1.0 V. Then the electric outputs of the TENG network under the transverse impulse waves and longitudinal impulse waves were measured and presented in Figures S1 and S2 (Supporting Information). The similar tendencies of the current, voltage, and power with respect to the water wave amplitude were observed for the two water wave types. These indicate that larger wave amplitude is beneficial to produce higher performance of TENG network device. For comparison, Figure 3d shows the output power–resistance relationships under the three types of water waves, where the value of H_{out} is unified at 2.5 V. For different water wave types, the optimal frequencies for getting the maximum peak power are not fully consistent.

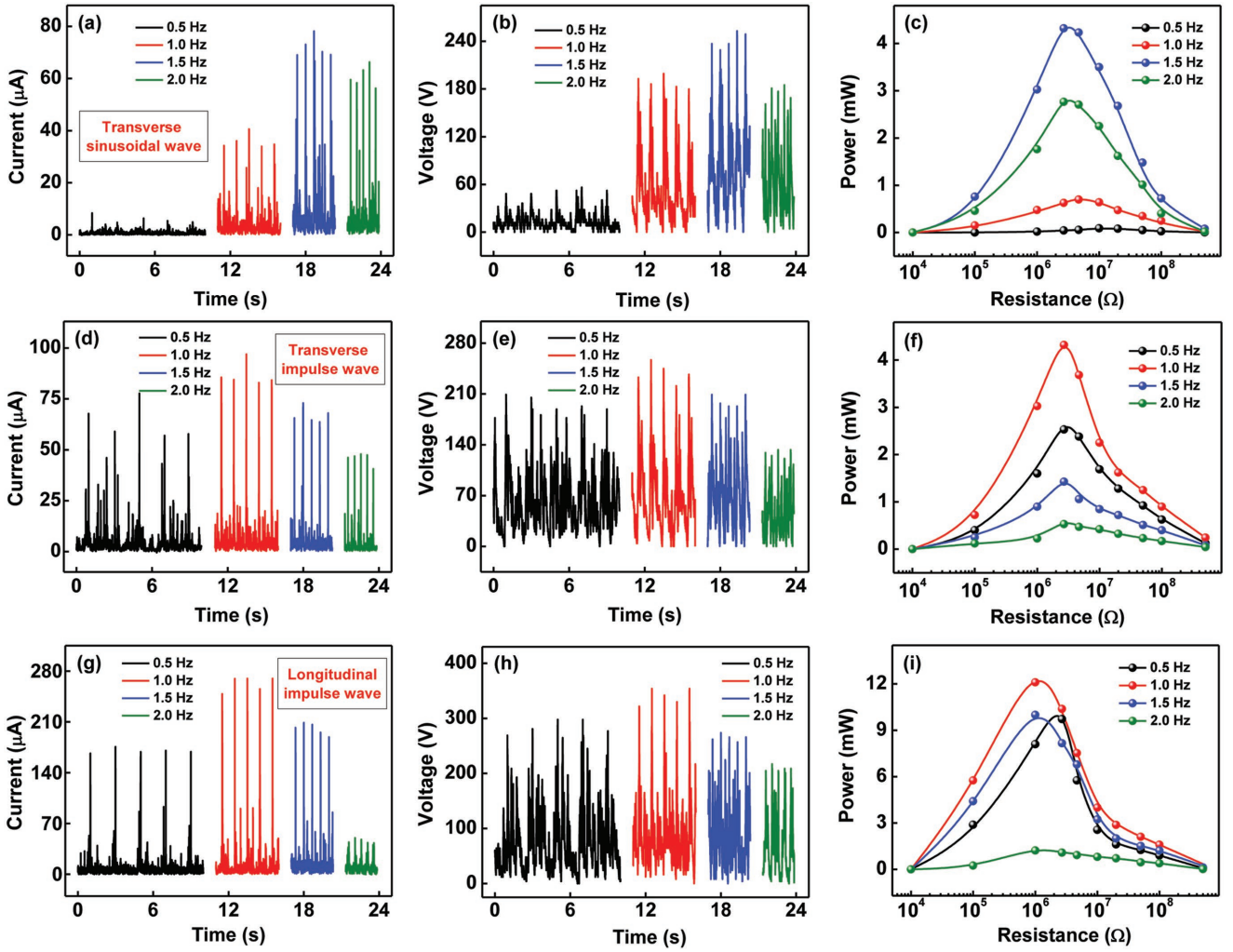

Figure 2. a) Output current, b) output voltage, and c) instantaneous output power–resistance profiles of the hexagonal TENG network at various frequencies under the transverse sinusoidal waves. d) Output current, e) output voltage, and f) output power–resistance profiles of the TENG network at various frequencies under the transverse impulse waves. g) Output current, h) output voltage, and i) output power–resistance relationships of the TENG network at various frequencies under the longitudinal impulse waves. The output amplitude of function generator was fixed as 2.5 V.

Because the matched resistance of TENG is closely associated with the motion frequency, the matched resistance changes with the water wave type. The longitudinal impulse waves drive the TENG network to generate the highest output power which can be also viewed in Figure 2. Besides the hexagonal TENG network, we also fabricated a TENG network with nine units arranged in a 3×3 square. Under the same experimental conditions employed, the outputs are relatively lower (265 μA, 314 V, and 8.12 mW), as shown in Figure S3 (Supporting Information). It implies the unit number in the network can have an effect on the output performance of the network. In this work, we mainly considered the hexagonal TENG network, and the unit number and the arrangement manner will be carefully studied in future.

To achieve extensive applications of TENG network in harvesting water wave energy, we implemented an efficient and autonomous PMM to manage the harvested electric energy. The PMM has a compact package in size of $2 \times 1 \times 1$ cm^3, which is very suitable for integrating with the TENG network. The schematic diagram of the power management mechanism on the TENG network is demonstrated in **Figure 4**a, which is an AC–DC buck conversion circuit by coupling TENG network, rectifiers, and classical DC–DC buck converter. The integrating of these components including rectifier bridges, a switch, a parallel freewheeling diode *D*, a serial inductor *L*, and a parallel capacitor *C* can realize the maximized energy transfer and the DC buck conversion.[37] In the implemented PMM, a micropower voltage comparator and a metal-oxide-semiconductor field effect transistor (MOSFET) were used to achieve the autonomous switching with self-management mechanism. Note that the TENG units in the network were respectively connected to a rectifier bridge followed by a series electrical connection. The series connection was used to instead of the general common parallel connection, because it could generate higher voltage and impedance for matching the PMM (Figure S4, Supporting Information).

Integrated with the PMM, the electric outputs of the TENG network were characterized as shown in Figure 4b–e. As an example, we measured the outputs for the hexagonal TENG network containing seven spherical TENG units linked through

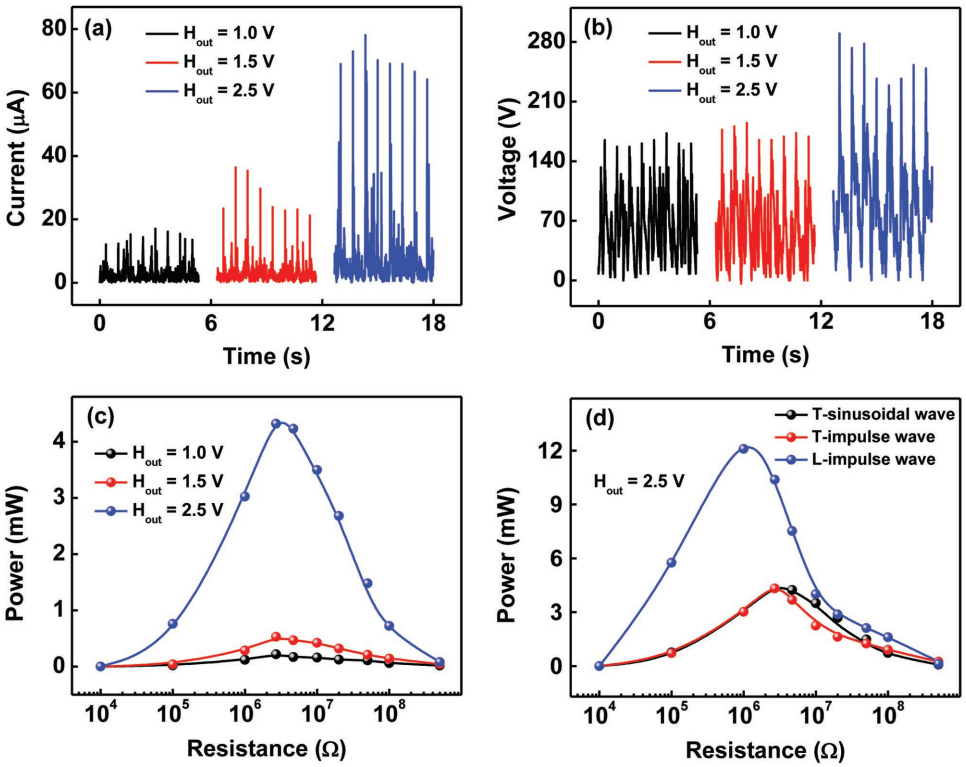

Figure 3. a) Output current, b) output voltage, and c) output power–resistance profiles of the hexagonal TENG network at various wave amplitudes (reflected by H_{out} of the instrument) under the transverse sinusoidal waves. The water wave frequency generated by the function generator was fixed at 1.5 Hz. d) Comparison for the output power of the network under three types of water waves at H_{out} = 2.5 V.

the cable ties under the longitudinal impulse waves at the frequency of 1.0 Hz and the amplitude of 2.5 V. The TENG units are electrically connected in series after the rectifier bridges. In the fabricated PMM, L = 5 mH and C = 100 μF are set. When loading a resistor, the voltage on the resistor continuously ascends from zero until reaching steady states, as shown in Figure 4b. The time for the voltage to reach the saturation is very short. We can also view the saturated voltage increase with increasing the load resistance (Figure 4d), that is from 0.9 to 10.1 V as the resistance varies from 10 kΩ to 1 GΩ. This trend is owing to the existence of internal impedance of the TENGs. The load occupies higher voltage at a larger resistance. In contrast, the ripples exhibit an obvious decrease with the resistance to realize the steady state condition of inductor volt-second balance, in which the average inductor voltage is zero for each circuit cycle.[37] It is obvious that the output voltage can meet the demands of traditional electronics.

Then the charging performance of the TENG network integrated with the PMM to a load capacitor was investigated. Figure 4c shows the charging voltage curves for different capacitors. For all capacitances, at zero time the capacitors are charged at the maximum speed and then the charging speeds slow gradually. The capacitor with a smaller capacitance can get a larger voltage and a higher charging speed. The voltages of the capacitors of 1 and 3.3 mF can be raised to 2.535 and 1.023 V within 60 s by the TENG network integrated with the PMM. The inset of Figure 4d indicates that the stored energy can reach the maximum of 4.285 mJ at an optimal capacitance of 470 μF within 60 s. For comparison between the managed and direct charging processes, the charging profiles of the TENG network for charging a 10 mF capacitor were characterized in the two processes. As shown in Figure 4e, by direct charging for 60 s, the voltage only increases from 0 to 0.035 V with an increment of 6.125 μJ. While the voltage increases from 0 to 0.345 V with an increment of 0.595 mJ by the PMM with 96 times improvement in stored energy. The similar characteristics can be found in charging 1 and 6.8 mF capacitors from zero voltage for the TENG network (Figure S5, Supporting Information). The stored energy can be enhanced by 46 and 66 times for the managed charging when respectively charging 1 and 6.8 mF capacitors. The charging speed can also be improved dramatically for a single spherical TENG unit of the network (Figure S6, Supporting Information).

To demonstrate the applications of the power-managed TENG network in powering portable electronics by harvesting the water wave energy, a digital thermometer and a wireless transmitter were chosen for example. A photograph of the thermometer driven by the TENG network integrated with the PMM under the transverse sinusoidal wave motions at 1.5 Hz through connecting a capacitor of 47 μF in parallel is shown in **Figure 5**a. The TENG units in the network linked by cable ties were connected with rectifier bridges, electrically connected in series, and then connected by the PMM. The sensor probe of the thermometer was placed below the water surface to detect the water temperature, and then these signals were displayed on the LCD screen. The experiment process of powering the thermometer

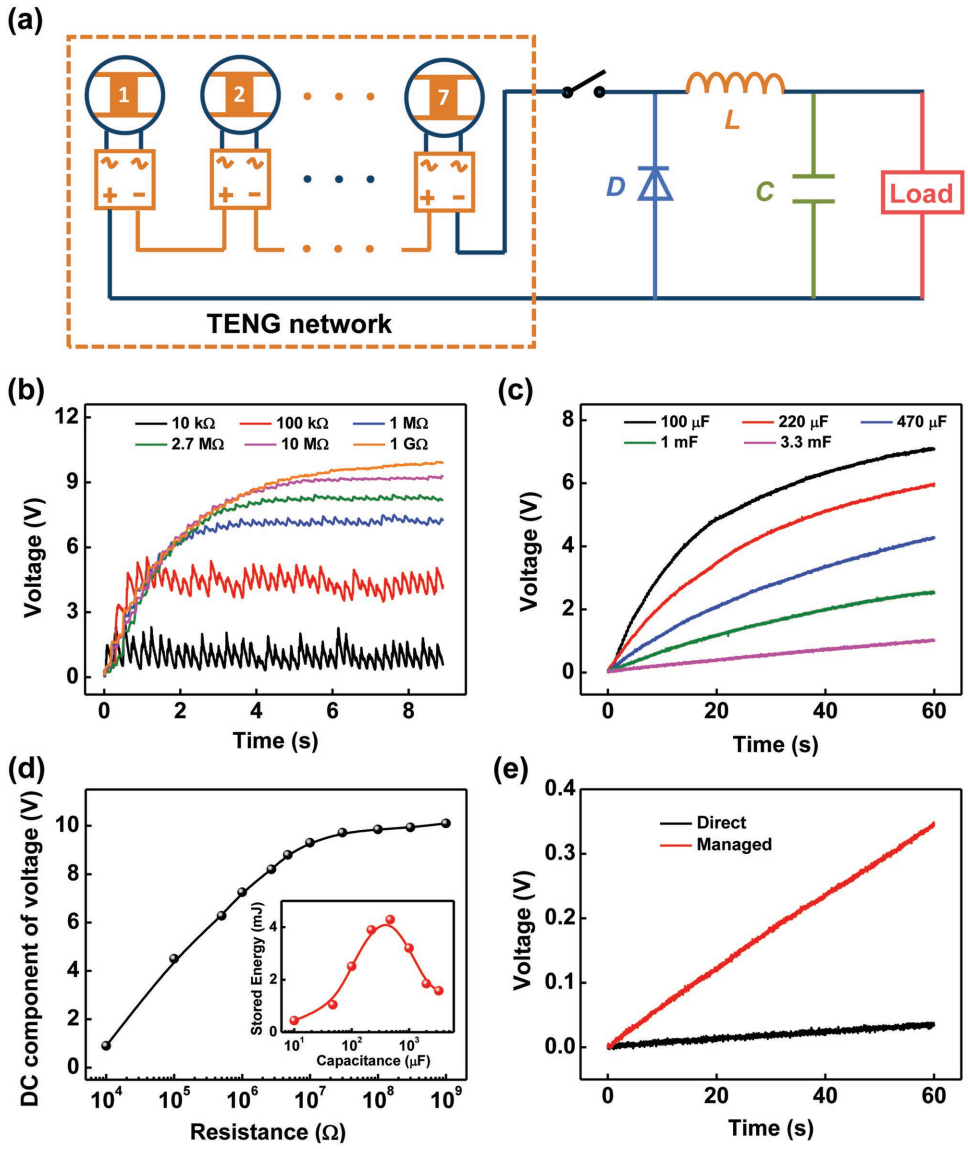

Figure 4. a) Schematic diagram of the power management mechanism for the TENG network in which the units are respectively connected to a rectifier bridge followed by a series electrical connection. b) Output voltage on a load resistor for the TENG network with the PMM at various resistances under the longitudinal impulse waves. c) Charging voltage curves for different capacitors. d) Extracted DC component of voltage with respect to the resistance, and calculated stored energy on the capacitor with the capacitance within 60 s. e) Comparison for the charging profiles of the TENG network between the managed charging and direct charging for a 10 mF capacitor.

is also shown in Video S2 (Supporting Information). At the first stage, the capacitor in the PMM and externally connected capacitor are charged and the thermometer does not work. When the voltage is large enough the thermometer is turned on, and then it can constantly measure the temperature. That can be reflected by the voltage profile on the thermometer when powered by the TENG network with the PMM, as shown in Figure 5b. The voltage increases gradually to around 1.2 V at about 18 s, where the thermometer is turned on and starts to work, and then the voltage stabilizes and fluctuates up and down 1.2 V. After the initial prestarting stage, the thermometer can work constantly as long as the water waves are generated.

Besides the digital thermometer, the TENG network with the PMM was also applied to drive a wireless transmitter, as shown in Figure 5c. The units in the network are still connected to rectifier bridges, respectively, and then electrically connected in series. The PMM is first integrated with a wireless transmitter module, and they are together connected by the TENG network. At the initial prestarting stage, the capacitor in the PMM is charged to a certain degree, and then the wireless transmitter is powered up to send signals through the antenna to the receiver placed at about 3 m away. Based on the signals the alarm is turned on and sent out sound and light (Video S3, Supporting Information). The wireless transmitter can send signals to the receiver at a long distance of above 10 m, but due to the space limitation, we only show the case for about 3 m away. Figure 5d shows the voltage variation of the transmitter connected with the PMM for several consequent transmitting cycles. The voltage

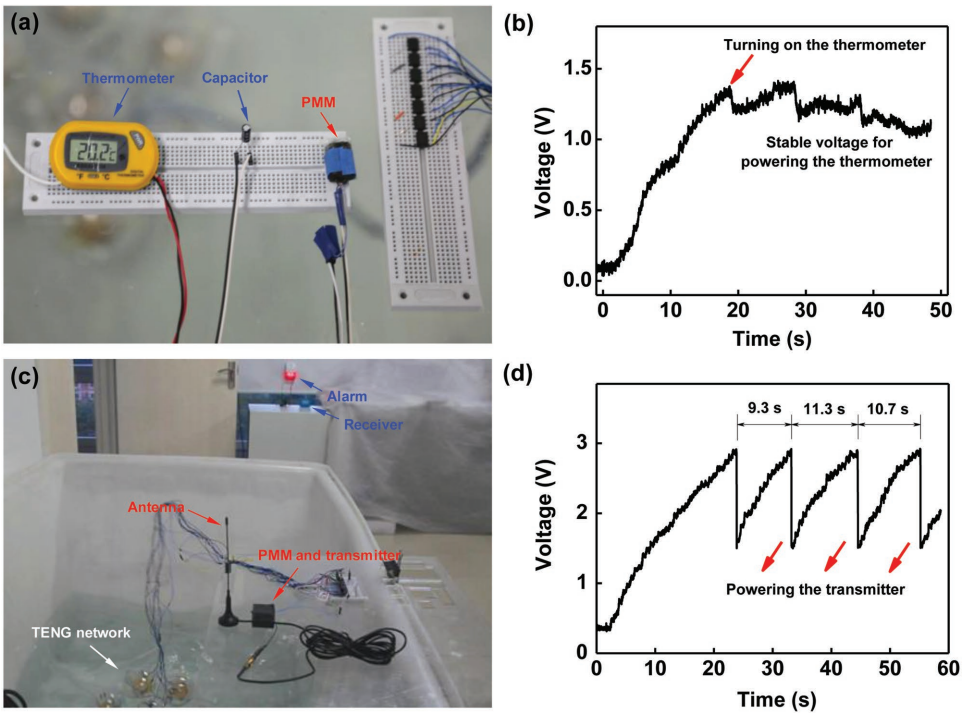

Figure 5. a) Photograph of a digital thermometer driven by the TENG network integrated with the PMM under the transverse sinusoidal wave motions through connecting a capacitor of 47 μF. b) The voltage profile on the digital thermometer when powered by the TENG network with the PMM. c) Photograph of a wireless transmitter powered by the TENG network with the PMM under the transverse sinusoidal waves, which sends a signal to the receiver to turn on the alarm. d) The voltage variation of the transmitter connected with the PMM for several consequent transmitting cycles.

increases rapidly to 2.9 V at about 23 s, and then the transmitter is driven to send signals for alarming. After the prestarting stage, the wireless transmitter can send signals for alarming once every 10 s, which is a dramatic improvement over the case without the PMM. Figure S7 (Supporting Information) is the voltage curve of two transmitting cycles through directly charging a 220 μF capacitor by the TENG network under the transverse sinusoidal waves, showing the time for transmitting once is about 160 s and the large improvement with the PMM.

3. Conclusion

In summary, we demonstrated a hexagonal TENG network consisting of spherical TENG units with spring-assisted multilayered structure and integrated it with the PMM for effectively harvesting the water wave energy. The influences of the water wave frequency and amplitude on the output performance of TENG network were investigated for the transverse sinusoidal waves, transverse impulse waves, and longitudinal impulse waves. The highest outputs of the TENG network were obtained at the frequency of 1.0 Hz and the amplitude of 2.5 V under the longitudinal impulse waves, reaching 270 μA, 354 V, and 12.20 mW, with the corresponding power density of 3.33 W m^{-3}. When integrated with the PMM, the TENG network with units connected in series could output a steady and continuous DC voltage on the load resistance, and the stored energy was greatly improved in charging a capacitor (96 times improvement for 10 mF capacitor). Finally, a digital thermometer and a wireless transmitter were successfully powered by the power-managed TENG network, showing the largely improved performance with the power management toward the blue energy application.

4. Experimental Section

Fabrication of the Hexagonal TENG Network: First, the spherical TENG units in the network were fabricated. For each spherical unit, a 50 μm thick Kapton strip (32 cm × 4 cm) served as the substrate of the multilayered TENG. The strip was evenly folded into eight squares (4 cm × 4 cm) and shaped into a zigzag structure. An Al foil (3 cm × 3 cm) and a 12.5 μm thick FEP film (3 cm × 3 cm) bonded by another Al foil were adhered on two adjacent intervals of the Kapton strip, and the Al side of FEP–Al film was attached by a flexible foam (3.2 cm × 3.2 cm) to improve the contact intimacy between triboelectric materials. Electrons were injected to the FEP surfaces to increase the surface charges at a polarization voltage of 5 kV. The design of the spring structure and other details can be found in the previous work.[35] Second, the sealing and waterproofing on the spherical TENG units were processed by using the tile cement. Third, seven spherical TENG units were respectively connected to a rectifier bridge, and then electrically connected in parallel. The cable ties were used to link the units into a hexagon network, including one unit arranged at the center of the hexagon and six units at the apexes of the hexagon. When the network with the PMM was integrated, the units were electrically connected in series to produce a higher voltage.

Electric Measurements of the TENG Device: The electric outputs of the TENG network were measured under the water waves generated by a series of wave pumps (rw-20 Jepower Technology Inc.) controlled by a

function generator (AFG3011C Tektronix Inc.). The output current of the TENG network and the voltage managed by the PMM were measured by a current preamplifier (Keithley 6514 System Electrometer), while the voltage directly outputted by the TENG network was measured by a digital oscilloscope (Agilent InfiniiVision 2000X).

Supporting Information

Supporting Information is available from the Wiley Online Library or from the author.

Acknowledgements

X.L., T.J., and G.L. contributed equally to this work. Supports from the National Key R & D Project from the Minister of Science and Technology (2016YFA0202704), the Beijing Municipal Science & Technology Commission (Z171100000317001), and the National Natural Science Foundation of China (Grant Nos. 51432005, 51702018, and 51561145021) were appreciated. The authors also thank Wei Tang, Kai Han, Yawei Feng, Jie An, Shaohang Xu, Wenbo Liu, and Xiaodan Yang for device fabrications and measurements.

Conflict of Interest

The authors declare no conflict of interest.

Keywords

blue energy, power management module, spring-assisted multilayered structure, triboelectric nanogenerator networks, water wave energy harvesting

Received: October 13, 2018
Revised: November 20, 2018
Published online:

[1] J. P. Painuly, *Renewable Energy* **2001**, *24*, 73.
[2] A. Khaligh, O. C. Onar, *Energy Harvesting: Solar, Wind, and Ocean Energy Conversion Systems*, CRC Press, Boca Raton, FL **2009**.
[3] Z. L. Wang, J. Chen, L. Lin, *Energy Environ. Sci.* **2015**, *8*, 2250.
[4] A. F. de, O. Falcao, *Renewable Sustainable Energy Rev.* **2010**, *14*, 899.
[5] Z. L. Wang, *Nature* **2017**, *542*, 159.
[6] S. H. Salter, *Nature* **1974**, *249*, 720.
[7] S. P. Beeby, R. N. Torah, M. J. Tudor, P. Glynne-Jones, T. O. Donnell, C. R. Saha, S. Roy, *J. Micromech. Microeng.* **2007**, *17*, 1257.
[8] J. Tollefson, *Nature* **2014**, *508*, 302.
[9] A. Von Jouanne, *Mech. Eng.* **2006**, *128*, 24.
[10] R. Henderson, *Renewable Energy* **2006**, *31*, 271.
[11] F.-R. Fan, Z.-Q. Tian, Z. L. Wang, *Nano Energy* **2012**, *1*, 328.
[12] C. Zhang, T. Zhou, W. Tang, C. B. Han, L. M. Zhang, Z. L. Wang, *Adv. Energy Mater.* **2014**, *4*, 1301798.
[13] Y. N. Xie, S. H. Wang, S. M. Niu, L. Lin, J. Yang, Z. Y. Wu, Z. L. Wang, *Adv. Mater.* **2014**, *26*, 6599.
[14] W. Tang, T. Jiang, F. R. Fan, A. F. Yu, C. Zhang, X. Cao, Z. L. Wang, *Adv. Funct. Mater.* **2015**, *25*, 3718.
[15] G. Zhu, Y. S. Zhou, P. Bai, X. S. Meng, Q. S. Jing, J. Chen, Z. L. Wang, *Adv. Mater.* **2014**, *26*, 3788.
[16] T. Jiang, X. Chen, C. B. Han, W. Tang, Z. L. Wang, *Adv. Funct. Mater.* **2015**, *25*, 2928.
[17] C. B. Han, C. Zhang, J. Tian, X. Li, L. Zhang, Z. Li, Z. L. Wang, *Nano Res.* **2015**, *8*, 219.
[18] S. H. Wang, Y. N. Xie, S. M. Niu, L. Lin, Z. L. Wang, *Adv. Mater.* **2014**, *26*, 2818.
[19] S. H. Wang, S. M. Niu, J. Yang, L. Lin, Z. L. Wang, *ACS Nano* **2014**, *8*, 12004.
[20] C. B. Han, W. M. Du, C. Zhang, W. Tang, L. M. Zhang, Z. L. Wang, *Nano Energy* **2014**, *6*, 59.
[21] Y. Bian, T. Jiang, T. Xiao, W. Gong, X. Cao, Z. Wang, Z. L. Wang, *Adv. Mater. Technol.* **2018**, *3*, 1700317.
[22] J. Chen, J. Yang, Z. L. Li, X. Fan, Y. L. Zi, Q. S. Jing, H. Y. Guo, Z. Wen, K. C. Pradel, S. M. Niu, Z. L. Wang, *ACS Nano* **2015**, *9*, 3324.
[23] X. F. Wang, S. M. Niu, Y. J. Yin, F. Yi, Z. You, Z. L. Wang, *Adv. Energy Mater.* **2015**, *5*, 1501467.
[24] T. X. Xiao, T. Jiang, J. X. Zhu, X. Liang, L. Xu, J. J. Shao, C. L. Zhang, J. Wang, Z. L. Wang, *ACS Appl. Mater. Interfaces* **2018**, *10*, 3616.
[25] L. Xu, Y. Pang, C. Zhang, T. Jiang, X. Chen, J. Luo, W. Tang, X. Cao, Z. L. Wang, *Nano Energy* **2017**, *31*, 351.
[26] T. Jiang, L. M. Zhang, X. Y. Chen, C. B. Han, W. Tang, C. Zhang, L. Xu, Z. L. Wang, *ACS Nano* **2015**, *9*, 12562.
[27] T. Jiang, Y. Yao, L. Xu, L. Zhang, T. Xiao, Z. L. Wang, *Nano Energy* **2017**, *31*, 560.
[28] L. Zhang, C. B. Han, T. Jiang, T. Zhou, X. Li, C. Zhang, Z. L. Wang, *Nano Energy* **2016**, *22*, 87.
[29] Y. Yao, T. Jiang, L. Zhang, X. Chen, Z. Gao, Z. L. Wang, *ACS Appl. Mater. Interfaces* **2016**, *8*, 21398.
[30] L. Feng, G. Liu, H. Guo, Q. Tang, X. Pu, J. Chen, X. Wang, Y. Xi, C. Hu, *Nano Energy* **2018**, *47*, 217.
[31] Z. L. Wang, *Mater. Today* **2017**, *20*, 74.
[32] Z. L. Wang, T. Jiang, L. Xu, *Nano Energy* **2017**, *39*, 9.
[33] Y. L. Zi, H. Guo, Z. Wen, M.-H. Yeh, C. Hu, Z. L. Wang, *ACS Nano* **2016**, *10*, 4797.
[34] Z. L. Wang, *Faraday Discuss.* **2014**, *176*, 447.
[35] L. Xu, T. Jiang, P. Lin, J. Shao, C. He, W. Zhong, X. Chen, Z. L. Wang, *ACS Nano* **2018**, *12*, 1849.
[36] T. X. Xiao, X. Liang, T. Jiang, L. Xu, J. J. Shao, J. H. Nie, Y. Bai, W. Zhong, Z. L. Wang, *Adv. Funct. Mater.* **2018**, *28*, 1802634.
[37] F. B. Xi, Y. K. Pang, W. Li, T. Jiang, L. M. Zhang, T. Guo, G. X. Liu, C. Zhang, Z. L. Wang, *Nano Energy* **2017**, *37*, 168.
[38] S. M. Niu, X. F. Wang, F. Yi, Y. S. Zhou, Z. L. Wang, *Nat. Commun.* **2015**, *6*, 8975.
[39] H. Hou, Q. Xu, Y. Pang, L. Li, J. Wang, C. Zhang, C. Sun, *Adv. Sci.* **2017**, *4*, 1700072.
[40] K. R. Wijewardhana, T. K. Ekanayaka, E. N. Jayaweera, A. Shahzad, J. K. Song, *Energy* **2018**, *160*, 648.